Front. Struct. Civ. Eng. 2018, 12(1): 44–57
https://doi.org/10.1007/s11709-016-0382-6

RESEARCH ARTICLE

A hybrid LQR-PID control design for seismic control of buildings equipped with ATMD

Amir Hossein HEIDARI[a], Sadegh ETEDALI[b*], Mohamad Reza JAVAHERI-TAFTI[a]

[a] *Department of Civil Engineering, Taft Branch, Islamic Azad University, Taft, Iran*

[b] *Department of Civil Engineering, Birjand University of Technology, P.O. Box 97175-569, Birjand, Iran*

[*] *Corresponding author. E-mail: etedali@birjandut.ac.ir*

ABSTRACT This paper presents an efficient hybrid control approach through combining the idea of proportional-integral-derivative (PID) controller and linear quadratic regulator (LQR) control algorithm. The proposed LQR-PID controller, while having the advantage of the classical PID controller, is easy to implement in seismic-excited structures. Using an optimization procedure based on a cuckoo search (CS) algorithm, the LQR-PID controller is designed for a seismic- excited structure equipped with an active tuned mass damper (ATMD). Considering four earthquakes, the performance of the proposed LQR-PID controller is evaluated. Then, the results are compared with those given by a LQR controller. The simulation results indicate that the LQR-PID performs better than the LQR controller in reduction of seismic responses of the structure in the terms of displacement and acceleration of stories of the structure.

KEYWORDS seismic control, tuned mass dampers, cuckoo search, PID controller, LQR controller

1 Introduction

Vibration control devices can be classified as passive, active, semi-active and hybrid control devices. Vibration control of structure is one area of current research that focuses on mitigation of structural vibrations during earthquakes and strong winds [1].

Tuned mass dampers (TMDs) are the oldest passive seismic control devices, which are tuned with a vibration frequency close to the fundamental frequency of structure. Because of the uncertainty in the estimation of parameters of the structure, accurate determination of the natural frequency of the structure is not possible. This frequency also varies in the face of strong dynamic loads, such as earthquakes and strong winds. Therefore, the performance of these systems because of its constant dynamic parameters is limited and these systems can only provide a favorable performance in a narrow range of load frequencies. In over to overcome these shortcomings, active tuned mass dampers (ATMDs) are suggested [2]. In a structure equipped with ATMD, an actuator, which is placed between the structure and the TMD system, applies a control force in real time to the ATMD and its reaction applied to the structure. The adopted control algorithm for tuning the control force has a key role in successful implementation of ATMDs. An effective control algorithm can create a suitable trade-off between two conflicting objective of reducing control force and reducing structural responses. Considering the structures equipped with ATMD, different control algorithms are employed. The most common control algorithms for this case are LQR, linear quadratic Gaussian (LQG), H_∞, fuzzy logic controller [3–8].

Despite the recent advances in control methods, because of the significant effectiveness and simplify implementation of the classical PID controllers, they are widely used in various engineering applications. Due to these advantages, PID controllers have been applied by several researchers for vibration control of plates and beams [9–11]. Furthermore, in the area of structural control, several researchers attempt to apply the PID controller toward seismic control of structures [12–15]. Aguirre et al. [16] suggested a proportional-integral (PI) controller to minimize the structural vibrations of a 3-story building equipped with MR dampers. Optimal PD/PID controllers using genetic algorithm are developed by Etedali et al. [17]

Article history: Received Jun 10, 2016; Accepted Sept 18, 2016

for seismic control of a benchmark isolated structure equipped with piezoelectric friction dampers. Also, they proposed an independent robust modal PID control approach for seismic control of buildings [18]. Subasri et al. [19] proposed a control scheme based on a combination of discrete PID controller and discrete direct adaptive neural controller. The effect of feedback on PID controlled active structures was considered by Nigdeli [20]. Yu et al. [21] used the standard industrial proportional-derivative (PD) and PID controllers for active vibration control of a structure equipped with ATMD. Recently, Etedali et al. [22] proposed a new design method based on decoupling of PID controller for seismic control of smart structures.

LQR controller is one of the most famous and practical control algorithms for solving control problems. This controller used by researchers at the beginning of research in the area of seismic control. Several modifications are still done to enhance the performance of the traditional LQR algorithm for application toward the structural vibration control [23–28].

Since the process of seismic control of structures is basically a multi-input multi-output process, the LQR controller can easily be implemented, in the state space, for seismic control of structures. However, in the case of structural control, the off-diagonal terms in damping and stiffness matrices of the structures cause the cross coupling of the process channels. This issue makes it difficult to implement of classical controllers such as PID controller for seismic control of structures. Considering this issue, the present paper proposes a new design of PID controller based on the LQR controller. This controller is named the LQR-PID controller. The proposed controller, while having the advantage of the classical PID control, is easy to implement in seismic-excited structures. When the velocity vector of story is the feedback signal of the controller, the differential term of the proposed controller reduces floor acceleration and the integration term considers the reduction in floor displacement. In fact, the structure of PID controller plays a vital role in the simultaneous reduction of the structural responses in the terms of the maximum displacement and acceleration of stories. The problem of LQR-PID control design for seismic control of structures forms an optimization problem. To solve this problem, a meta-heuristic optimization algorithm keeping enough diversity of the population is required. Compared with the genetic algorithms (GA), particle swarm optimization (PSO) and ant colony optimization (ACO) algorithms, the cuckoo search (CS) is able to explore the search space more accurately and can perform better for challenging objective functions [29–32]. Hence, we suggested the use of CS algorithm as a powerful tool for optimization problems. In order to prove the validity of the proposed controller, a 10-story structure equipped with an ATMD is considered. Four well-known earthquake records are adopted to evaluate the performance of the proposed control strategy in different load disturbance. In comparison with LQR, the performance of the LQR-PID controller in reduction of seismic responses is validated.

The paper is organized as follows. An overview of structural model is presented in Sections 2. Brief overviews of LQR and PID controllers are introduced in Section 3 and 4, respectively. Control system design using LQR-PID control approach is developed in Section 5. The optimization procedure using CS algorithm is explained in Section 6. Numerical studies are carried out on a 10 story building in Section 7. Furthermore, the simulation results are discussed in this Section. At the end, the concluding remarks are drawn.

2 The mathematical equation of motion of structures

The dynamic equation of motion of an n-story shear frame structure, subject to ground acceleration, $\ddot{x}_g(t)$, can be expressed as follows:

$$\mathbf{M}\ddot{\mathbf{x}}(t) + \mathbf{C}\dot{\mathbf{x}}(t) + \mathbf{K}\mathbf{x}(t) = -\mathbf{M}\mathbf{\Lambda}\ddot{x}_g(t), \tag{1}$$

where $\mathbf{M}$, $\mathbf{C}$, and $\mathbf{K}$ are the $n \times n$ mass, damping, and stiffness matrices of the structure, respectively. $\mathbf{x}(t)$ is the $n \times 1$ relative displacement vector of the floors with respect to the ground. The $n \times 1$ vector indicates the location of the earthquake load applied to the structure.

For a smart structure, the control force vector $\mathbf{u}(t)$ is entered to the equation of motion of the structure. Therefore, the equation of motion of a smart structure is given by Eq. (2).

$$\mathbf{M}\ddot{\mathbf{x}}(t) + \mathbf{C}\dot{\mathbf{x}}(t) + \mathbf{K}\mathbf{x}(t) = -\mathbf{M}\mathbf{\Lambda}\ddot{\mathrm{x}}_g(t) + \mathbf{D}\mathbf{u}(t), \tag{2}$$

where matrix $\mathbf{D}$ is the $n \times n_c$ location matrix of the control forces.

The dynamic behavior of many systems can concurrently be expressed with a first order differential equation:

$$\dot{\mathbf{z}}(t) = g(\mathbf{z}(t), \mathbf{u}(t), t), \tag{3}$$

in which, t is time, $\mathbf{z}(t)$ is the state vector of the system, and $\mathbf{u}$(t) is the output vector of the controller. In many systems, the state vector is selected with respect to the physical nature of the system. Vector $\mathbf{z}(t)$ can be selected as the following form for the structures:

$$\mathbf{z}(t) = \begin{Bmatrix} \mathbf{x}(t) \\ \dot{\mathbf{x}}(t) \end{Bmatrix}. \tag{4}$$

Therefore, the dynamic equations of motion of the structure in the state space form can be expressed as Eq. (5):

$$\dot{\mathbf{z}}(t) = \mathbf{A}\mathbf{z}(t) + \mathbf{B}\mathbf{u}(t) + \mathbf{H}\ddot{x}_g(t), \tag{5}$$

in which the state matrix **A**, input matrix **B** and vector **H** are given by Eq. (6).

$$\mathbf{A}=\begin{bmatrix}\mathbf{0}_{n\times n} & \mathbf{I}_{n\times n}\\ -\mathbf{M}^{-1}\mathbf{K} & -\mathbf{M}^{-1}\mathbf{C}\end{bmatrix},\ \mathbf{B}=\begin{bmatrix}\mathbf{0}_{n\times n_c}\\ \mathbf{M}^{-1}\mathbf{D}\end{bmatrix},\ \mathbf{H}=\begin{bmatrix}\mathbf{0}_{n\times 1}\\ -\mathbf{\Lambda}\end{bmatrix}. \tag{6}$$

3 LQR controller

LQR controller is one of the most commonly-used techniques to design of control system in seismic-excited structures. This technique can be used for both active and semi-active controls of buildings. In this controller, the optimal control forces are determined by minimizing the following cost function:

$$\mathrm{J}=\int_0^{t_\mathrm{d}}[\mathbf{z}^{\mathrm{T}}(t)\mathbf{Q}\mathbf{z}(t)+\mathbf{u}^{\mathrm{T}}(t)\mathbf{R}\mathrm{u}(t)]\mathrm{d}t, \tag{7}$$

where t_d is the time interval of interest. Also, the symmetric weighting matrices **Q** and **R** are the design parameters to obtain the required performance. The active control forces are given by Eq. (8).

$$\mathbf{u}(t)=-\mathbf{G}\mathbf{z}(t), \tag{8}$$

where **G** is a feedback gain matrix. This matrix is obtained as

$$\mathbf{G}=\mathbf{R}^{-1}\mathbf{B}^{T}\mathbf{P}, \tag{9}$$

where **P** is semi-positive definite matrix obtained from the Riccati equation. Because of simplicity in the structure and its implementation, LQR controller is the most popular controller among the optimal feedback control algorithm. But, the main disadvantage of the algorithm are the limitation of the number of sensors installed for measuring the state variables as well as the high complexity in determination of the weighting matrices in tall building [7].

4 An overview of PID controller

PID controller is a generic control loop feedback controller broadly applied in industrial control systems. A block diagram of a PID controller in a feedback loop is shown in Fig. 1.

$g(s)$ is the transfer function of the plant, $y(t)$ is the output of the system representing the structural response, $u(t)$ is the output of the controller i.e., the PID control force, $d(t)$ is the load (input) disturbance applied to the system simulating an earthquake dynamic force, $y_{\mathrm{ref}}(t)$ is the desired feedback of the structural response. Also, $e(t)$ is the error which is the difference between the reference value and the value of the output. It is common assumed $y_{\mathrm{ref}}(t)=0$ for structural control, therefore, $\mathrm{e}(t)=-y(t)$. Furthermore, G_P, G_I and G_D are the proportional, integral and derivative terms, respectively .As can be seen, the control force, $u(t)$, is determined using Eq. (10).

$$u(t)=G_\mathrm{P}e(t)+G_\mathrm{I}\int_0^t e(t)\mathrm{d}t+G_\mathrm{D}\frac{\mathrm{d}e(t)}{\mathrm{d}t}. \tag{10}$$

The proportional, integral and derivative terms of the PID controller are defined as $G_\mathrm{P}=k_c$, $G_\mathrm{I}=k_\mathrm{c}/\tau_\mathrm{i}$ and $G_\mathrm{D}=k_\mathrm{c}\tau_\mathrm{d}$ where k_c is the proportional gain, τ_i is the integral time, and τ_d is the derivative time. Also, the parameter t is the duration of the control process. Considering these definitions, the PID control force in the S and time domains are determined using Eq. (11) and (12), respectively.

$$k(s)=k_\mathrm{c}\left(1+\frac{1}{\tau_\mathrm{i}\mathrm{s}}+\tau_\mathrm{d}\mathrm{s}\right), \tag{11}$$

$$u(t)=k_\mathrm{c}\left[e(t)+\frac{1}{\tau_\mathrm{i}}\int_0^t e(t)\mathrm{d}t+\tau_\mathrm{d}\frac{\mathrm{d}e(t)}{\mathrm{d}t}\right]. \tag{12}$$

As soon as an error is detected, the proportional term takes immediate corrective action. Using only proportional controller, however, a steady state error occurs after a change in the load disturbance. The integral term can eliminate the steady state error. But, a disadvantage of integral action is that it tends to have a destabilizing effect. The derivative mode tends to stabilize the closed-loop system and increase the damping of the system. However,

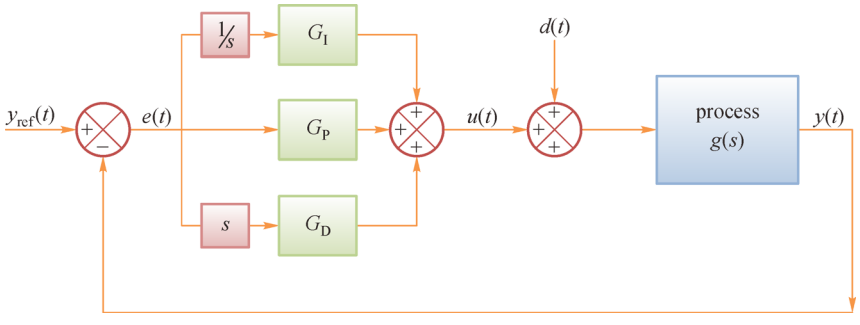

Fig. 1 A block diagram of a PID controller in a feedback loop

using the derivative action often leads to large control actions [17].

Considering the PID control force, described in Eq. (10), the control force vector of the structure, $\boldsymbol{u}(t)$, can be expressed as

$$\mathbf{u}(t) = -\mathbf{G}_{\mathrm{c}}\mathbf{W}_{\mathrm{c}}(t). \tag{13}$$

in which $\mathbf{G}_{\mathrm{c}}$ refer to $n_{\mathrm{c}} \times 3n_{\mathrm{c}}$ feedback gain matrix and $\mathbf{W}_{\mathrm{c}}(t)$ is a $3n_{\mathrm{c}} \times 1$ feedback vector of the controller. Also, n_{c} represents the number of actuators, i.e., the number of controlled stories. When the displacement vector of the controlled stories is adopted as feedback signal of control system, $\mathbf{G}_{\mathrm{c}}$ and $\mathbf{W}_{\mathrm{c}}(t)$ are given by

$$\begin{aligned} \mathbf{G}_{\mathrm{c}} &= \begin{bmatrix} \mathbf{G}_{\mathrm{I_c}} & \mathbf{G}_{\mathrm{P_c}} & \mathbf{G}_{\mathrm{D_c}} \end{bmatrix}, \\ \mathbf{W}_{\mathrm{c}}(t) &= \left[\int \mathbf{x}_{\mathrm{c}}(t) \mathbf{x}_{\mathrm{c}}(t) \dot{\mathbf{x}}_{\mathrm{c}}(t) \right]^{\mathrm{T}}, \end{aligned} \tag{14}$$

where $\mathbf{G}_{\mathrm{I_c}}$,$\mathbf{G}_{\mathrm{P_c}}$ and $\mathbf{G}_{\mathrm{D_c}}$ are $n_{\mathrm{c}} \times n_{\mathrm{c}}$ matrices. Moreover, $\mathbf{x_c}(t)$ refer to $n_{\mathrm{c}} \times 1$ displacement vector of the controlled stories, respectively.

5 The proposed LQR-PID control approach

In this section, through combining the idea of PID controller and LQR control theory, a hybrid modal LQR-PID control design is proposed. Then, the gain feedback matrix of the control system is designed according to the contribution of the modal responses to the structural response.

A set of n simultaneous differential equations forms Eq. (2), which is coupled by the off-diagonal terms in the stiffness and damping matrices. Using the coordinate transformations as $\mathbf{x}(t) = \boldsymbol{\Phi}\mathbf{y}(t)$, theses equations are transformed into a set of n independent normal coordinate equations in the modal space, in which $\mathbf{y}(t)=[y_1(t), y_2(t), \ldots, y_n(t)]^{\mathrm{T}}$ is the modal displacement vector and $\boldsymbol{\Phi}$ is an $n \times n$ orthonormalized mode shape matrix relative to the mass matrix. In this case, considering the term $\boldsymbol{\Phi}^{\mathrm{T}}\mathbf{M}\mathbf{r}\ddot{x}_{\mathrm{g}}(t)$ as the load disturbance, which must be applied to the structure, Eq. (5) can be rewritten in the state space as follows [18]:

$$\begin{bmatrix} \dot{\mathbf{y}}(t) \\ \ddot{\mathbf{y}}(t) \end{bmatrix} = \begin{bmatrix} \mathbf{0}_{n\times n} & \mathbf{I}_{n\times n} \\ -\boldsymbol{\Omega}^2 & -\mathbf{C}_m \end{bmatrix} \begin{bmatrix} \mathbf{y}(t) \\ \dot{\mathbf{y}}(t) \end{bmatrix} + \begin{bmatrix} \mathbf{0}_{n\times n} \\ \mathbf{I}_{n\times n} \end{bmatrix} \mathbf{u}_m(t), \tag{15}$$

where $\boldsymbol{\Omega} = \mathrm{diag}(\omega_1,\ldots,\omega_i,\ldots,\omega_n)$ and $\mathbf{C}_m = \mathrm{diag}(2\xi_1\omega_1,\ldots, 2\xi_i\omega_i,\ldots,2\xi_n\omega_n)$. Parameters ω_i and ξ_i are the natural frequency and modal damping ratio of the ith mode. Also, $\mathbf{u}_m(t)$ is an $n \times 1$ modal control force vector, given by Eq. (16).

$$\mathbf{u}_m(t) = \boldsymbol{\Phi}^{\mathrm{T}}\mathbf{D}\mathbf{u}(t). \tag{16}$$

Considering Eq. (15), the state space equation of the ith mode of the structure is given by

$$\begin{bmatrix} \dot{y}_i(t) \\ \ddot{y}(t) \end{bmatrix} = \begin{bmatrix} 0 & 1 \\ -\omega_i^2 & -2\xi_i\omega_i \end{bmatrix} \begin{bmatrix} y_i(t) \\ \dot{y}_i(t) \end{bmatrix} + \begin{bmatrix} 0 \\ 1 \end{bmatrix} u_{mi}(t). \tag{17}$$

Considering the above equation, the transfer function of the structure in the ith mode and in the S domain can be expressed as the following second-order model [18]:

$$g_i(s) = \frac{1}{s^2 + 2\xi_i\omega_i + \omega_i^2}. \tag{18}$$

As shown in Fig. 1, the relationship between the input and output of the controller in the ith mode can be described as [18]

$$y_i(s) = g_i(s)k_i(s). \tag{19}$$

It is notable that the term $d(s)$, as the load disturbance, must be applied to the structure in each mode. Inserting Eq. (18) in Eq. (19), the following equation can be given

$$(s^2 + 2\xi_i\omega_i + \omega_i^2)y_i(s) = k_i(s). \tag{20}$$

By defining $e_i(t) = -y_i$, the above equation for the ith mode can be expressed as below:

$$\ddot{e}_i(t) + 2\xi_i\omega_i\dot{e}_i(t) + \omega_i^2 e_i(t) = -u_i(t). \tag{21}$$

Eq. (21) can be rewritten in the state space form as the following form:

$$\dot{\mathbf{w}}_i = \mathbf{A}_i\mathbf{w}_i + \mathbf{B}_i\mathbf{u}_i, \tag{22}$$

where

$$\mathbf{w}_i = \begin{pmatrix} \int e_i(t) \\ e_i(t) \\ \dot{e}_i(t) \end{pmatrix}, \ \mathbf{A}_i = \begin{pmatrix} 0 & 1 & 0 \\ 0 & 0 & 1 \\ 0 & -(\omega_i)^2 & -2\xi_i\omega_i \end{pmatrix}, \quad \mathbf{B}_i = \begin{pmatrix} 0 \\ 0 \\ -1 \end{pmatrix}. \tag{23}$$

Considering the traditional LQR algorithm, the following quadratic performance index, J_i is defined.

$$J_i = \int_0^t [\mathbf{w}_i^{\mathrm{T}}(t)\mathbf{Q}_i\mathbf{w}_i(t) + \mathrm{u}_i^{\mathrm{T}}(t)\mathrm{R}_i\mathrm{u}_i(t)]\mathrm{d}t, \tag{24}$$

where $\mathbf{Q}_i$ is the 3×3 weighting matrix for the ith modal state vector and R_i is the positive weighting factor for the corresponding modal control force, respectively. By

solving the Riccati equation, shown in Eq. (25), the modal LQR-PID control force can be obtained by Eq. (26).

$$\mathbf{A}_i^{\mathrm{T}}\mathbf{P}_i + \mathbf{P}_i\mathbf{A}_i\text{-}\mathbf{P}_i\mathbf{B}_i\mathrm{R}_i^{-1}\mathbf{B}_i^{\mathrm{T}}\mathbf{P}_i + \mathbf{Q}_i = \mathbf{0}, \tag{25}$$

$$u_i(t) = -\mathbf{G}_i\mathbf{w}_i(t). \tag{26}$$

With regard to the theory of the LQR controller, the ith modal control gain is obtained as:

$$\mathbf{G}_i = -R_i^{-1}\mathbf{B}_i^{\mathrm{T}}\mathbf{P}_i. \tag{27}$$

According to Eq. (27), the modal control force in the ith mode of the structure is calculated as:

$$\mathbf{G}_i = -R_i^{-1}[0\ \ 0\ \ -1]\begin{pmatrix} P_{11i} & P_{12i} & P_{13i} \\ P_{12i} & P_{22i} & P_{23i} \\ P_{13i} & P_{23i} & P_{33i} \end{pmatrix}$$

$$= R_i^{-1}[P_{13i}\ \ P_{23i}\ \ P_{33i}\ ] = [G_{\mathrm{I}i}\ \ G_{\mathrm{P}i}\ \ G_{\mathrm{D}i}]. \tag{28}$$

Considering the form of the PID controller, the modal control force in the ith mode of the structure can be stated as:

$$u_i(t) = -\mathbf{G}_i\mathbf{w}_i(t)$$

$$= G_{\mathrm{I}i}\int e_i(t)\mathrm{d}t + G_{\mathrm{P}i}e_i(t) + G_{\mathrm{D}i}\frac{\mathrm{d}e_i(t)}{\mathrm{d}t}. \tag{29}$$

Eq. (29) clearly indicates that with judicious select of the weighting matrix $\mathbf{Q}_i$ and the weighting factor R_i, a PID controller can easily be designed which preserves the defined performance of an LQR i.e., minimum the structural responses and the controller effort, simultaneously.

The lower order modes of a structure subjected to seismic excitations usually provide the greatest contribution to the structural responses. Thus, it is reasonable to truncate analysis when the number of modes is sufficient. In other words, a control system can be designed based on the reduced modal space. By considering only n_{mc} ($n_{\mathrm{mc}} < n$) mode of the structure and determining the control modal force at each selected mode of the structure, the gain feedback matrix of the proposed LQR-PID controller is obtained according to the contribution of the modal responses to the structural response as the following equation [22]:

$$\mathbf{G}_{\mathrm{c}} = \begin{cases} \mathbf{L}^{-1}\mathbf{G}_{\mathrm{mc}}\boldsymbol{\Psi}^{-1}, & \text{if } n_{\mathrm{mc}} = n_{\mathrm{c}}, \\ (\mathbf{L}^T\mathbf{L})^{-1}\mathbf{L}^T\mathbf{G}_{\mathrm{mc}}\boldsymbol{\Psi}^T(\boldsymbol{\Psi}\boldsymbol{\Psi}^T)^{-1}, & \text{if } n_{\mathrm{mc}} > n_{\mathrm{c}}, \\ \mathbf{L}^{\mathrm{T}}(\mathbf{L}\mathbf{L}^{\mathrm{T}})^{-1}\mathbf{G}_{\mathrm{mc}}(\boldsymbol{\Psi}^T\boldsymbol{\Psi})^{-1}\boldsymbol{\Psi}^{\mathrm{T}}, & \text{if } n_{\mathrm{mc}} < n_{\mathrm{c}}, \end{cases} \tag{30}$$

where $\mathbf{L} = \boldsymbol{\Phi}_{\mathrm{mc}}^{\mathrm{T}}\mathbf{D}$ is the modal participation matrix in which $\boldsymbol{\Phi}_{\mathrm{mc}}$ is an $n \times n_{\mathrm{mc}}$ matrix of the first n_{mc} modes of mode shape matrix $\boldsymbol{\Phi}$. Also, $\boldsymbol{\Psi}$ is a $3n_{\mathrm{c}} \times 3n_{\mathrm{mc}}$ matrix defined as

$$\boldsymbol{\Psi} = \begin{bmatrix} \boldsymbol{\varphi}_{n_{\mathrm{c}}\times n_{\mathrm{mc}}} & \mathbf{0}_{n_{\mathrm{c}}\times n_{\mathrm{mc}}} & \mathbf{0}_{n_{\mathrm{c}}\times n_{\mathrm{mc}}} \\ \mathbf{0}_{n_{\mathrm{c}}\times n_{\mathrm{mc}}} & \boldsymbol{\varphi}_{n_{\mathrm{c}}\times n_{\mathrm{mc}}} & \mathbf{0}_{n_{\mathrm{c}}\times n_{\mathrm{mc}}} \\ \mathbf{0}_{n_{\mathrm{c}}\times n_{\mathrm{mc}}} & \mathbf{0}_{n_{\mathrm{c}}\times n_{\mathrm{mc}}} & \boldsymbol{\varphi}_{n_{\mathrm{c}}\times n_{\mathrm{mc}}} \end{bmatrix}, \tag{31}$$

where $\boldsymbol{\varphi}$ is an $n_{\mathrm{c}}\times n_{\mathrm{mc}}$ matrix obtained from removing the rows corresponding to the uncontrolled stories of the matrix Φ_{mc}. Also, n_{c} is the number of the controlled stories of the structure. Furthermore, $\mathbf{G}_{\mathrm{mc}}$ is obtained as:

$$\mathbf{G}_{\mathrm{mc}} = \begin{bmatrix} \mathbf{G}_{\mathrm{I}_{\mathrm{mc}}} & \mathbf{G}_{\mathrm{P}_{\mathrm{mc}}} & \mathbf{G}_{\mathrm{D}_{\mathrm{mc}}} \end{bmatrix}, \tag{32}$$

in which $\mathbf{G}_{\mathrm{I}_{\mathrm{mc}}}$, $\mathbf{G}_{\mathrm{P}_{\mathrm{mc}}}$, and $\mathbf{G}_{\mathrm{D}_{\mathrm{mc}}}$ are $n_{\mathrm{mc}}\times n_{\mathrm{mc}}$ matrices formed as following:

$$\mathbf{G}_{\mathrm{I}_{\mathrm{mc}}} = \mathrm{diag}(G_{\mathrm{I}_1}, G_{\mathrm{I}_2}, ..., G_{\mathrm{I}_{n_{\mathrm{mc}}}}),$$

$$\mathbf{G}_{\mathrm{P}_{\mathrm{mc}}} = \mathrm{diag}(G_{\mathrm{P}_1}, G_{\mathrm{P}_2}, ..., G_{\mathrm{P}_{n_{\mathrm{mc}}}}), \tag{33}$$

$$\mathbf{G}_{\mathrm{D}_{\mathrm{mc}}} = \mathrm{diag}(G_{\mathrm{D}_1}, G_{\mathrm{D}_2}, ..., G_{\mathrm{D}_{n_{\mathrm{mc}}}}).$$

The modal control gains for the n_{mc} selected mode can be tuned using Eq. (28). Then, using Eqs. (33) and (32), the modal feedback gain matrix of the structure, $\mathbf{G}_{\mathrm{mc}}$, is formed and through substituting $\mathbf{G}_{\mathrm{mc}}$ in Eq. (30), the feedback gain matrix of controller, $\mathbf{G}_{\mathrm{c}}$, can be obtained. At the end, the control force vector of the structure, $\mathbf{u}(t)$, can be determined using Eq. (13) in real time.

Considering the structure equipped with an ATMD, $n_{\mathrm{c}} = 1$. It is notable that the statue of $n_{\mathrm{mc}} < n_{\mathrm{c}}$ in Eq. (30) does not exist for this case. On the other hand, it is common that at least three modes of the structures to be considered in the design of the controller. Therefore, Eq. (30) can be represented for the structure equipped with an ATMD as follows:

$$\mathbf{G}_{\mathrm{c}} = (\mathbf{L}^{\mathrm{T}}\mathbf{L})^{-1}\mathbf{L}^{\mathrm{T}}\mathbf{G}_{\mathrm{mc}}\boldsymbol{\Psi}^{\mathrm{T}}(\boldsymbol{\Psi}\boldsymbol{\Psi}^{\mathrm{T}})^{-1}. \tag{34}$$

6 The optimization procedure using cuckoo search algorithm

Cuckoo search is a stochastic metaheuristic algorithm that models the obligate brood parasitism of some cuckoo birds. CS has been introduced by Yang and Deb [33] to solve optimization problems. Two important features in this algorithm make CS superior to many other metaheuristic algorithms. First, Having infinite mean and variance, Lévy flights can explore the search space better than standard Gaussian processes. Secondly, CS restores a balance between local search and global search exploration. Some studies showed that CS provides a better performance than GA and PSO in terms of simplicity of algorithms, having less parameter to tune, and higher speed [29,30]. Also, a comparison between CS, PSO and ACO shows that CS gives more robust results [31].

The population size n, switching probability P_a, step-size α and the Lévy flights exponent β are configurable parameters of CS. Apart from the population size, the switching probability is the key parameter of the CS. Other parameters such as the Lévy flights exponent and step-size can be set as $\alpha = 0.1$ and $\beta = 1.5$ for most problems, p_a and n are variable and have great effects on the algorithm performance. A balance between local and global optimization is created by the switching probability. The probability for global optimization is reduced with increasing p_a and vice versa [29,33].

The steps of the standard CS algorithm can be described as follows [32,33]:

1) Each cuckoo lays one egg at a time and dumps it in a randomly chosen nest (crossover operator).

2) Number of nests that contain eggs with high quality will be transferred to the next generation (elitism).

3) The number of available host nests is fixed, and a host can discover an alien egg with a Probability p_a (mutation operator).

The first rule produces a new solution using a Lévy Flights and can be considered as a crossover operator. Outline of generating new solution via Lévy flight is summarized as below:

$$\mathbf{x}_i^{t+1} = \mathbf{x}_i^t + \boldsymbol{\alpha} \otimes \mathbf{L\acute{e}vy}(\beta), \tag{35}$$

where $\boldsymbol{\alpha} = \alpha_0 \otimes (x_j^t\text{-}x_i^t)$ and $\mathbf{L\acute{e}vy}(\beta) = u/|\nu|^{\frac{1}{\beta}}$. Here, $\boldsymbol{\alpha}$ is the step size parameter, α_0 is the step size scaling factor, $\mathrm{x_j^t}$ and $\mathrm{x_i^t}$ are two randomly selected solutions, $\mathbf{L\acute{e}vy}(\beta)$ is the step length which is produced according the Lévy Flights, and β is Lévy flights exponent. In addition, the parameters u and ν are given by the normal distributions as shown in Eq. (36). In this equation, Γ is the standard Gamma function.

$$\sigma_{\mathrm{u}} = \left\{ \frac{\Gamma(1+\beta)\sin(\pi\beta/2)}{\Gamma[(1+\beta)/2]\beta 2^{(\beta-1)/2}} \right\}^{1/\beta}, \ \sigma_{\mathrm{v}} = 1. \tag{36}$$

The second rule applies elitism strategy to accelerate convergence rate of CS. Finally, the third rule incorporates probabilistic strategy to replace not so good solutions. Indeed, it can be treated as a mutation search operator and prevents algorithm of being trapped in a local minimum. Eq. (37) indicates how a new solution can be generated by this search operator .

$$\mathbf{x}_i^{t+1} = \mathbf{x}_i^t + r \otimes H(p_{\mathrm{a}} - \varepsilon) \otimes (\mathbf{x}_j^t - \mathbf{x}_k^t). \tag{37}$$

In which H(u) represents the Heaviside function, ε and r are some random numbers with uniform distributions, and $\mathbf{x}_j^t$, $\mathbf{x}_k^t$ are two solutions that are selected randomly. The basic steps of the CS can be summarized as the pseudo code shown in Fig. 2.

7 Numerical studies

To evaluate the performance of the proposed controller, a 10-story structure with the same mass, stiffness and damping for all stories, respectively with the values of 357.24 tons, 654.98 MN/m, and 6.15 MN.s /m has been simulated. The main frequency of the structure has been calculated as 1.02 Hz. The optimum TMD parameters include the mass of TMD that is defined as α percent of the total mass of the structure, the ratio of frequencies or β that is obtained from dividing the natural frequency of the TMD by the main mode frequency of the structure, and ξ_{TMD} that is calculated as a percentage of the critical

```
Initialize a population of C host nests each with n solution x_i, i = 1, 2, ..., n
Calculate fitness value for each solution in each nest
while (stop condition = false)
        Get cuckoo X randomly
        for ith solution in X
            generate X_i^{t+1} solution by lévy flight [Eq. (35)]
         end for
        stochastically Choose a nest (say Y)
        for ith solution in X
              If (fitness(X_i^{t+1}) < fitness(Y_i))
                    replace solution Y_i by X_i^{t+1}
              end if
         end for
        throw out a fraction(p_a) of worse nests
        for each abandoned nest like K
              for ith solution in K
                    Generate K_i^{t+1} solutions by standard random walk [Eq. (37)]
               end for
        end for
        evalute new nests, Rank the solutions and find the current best
end while
```

Fig. 2 Pseudo code of CS

damping ratio of the structure. In order to achieve a practical design, a preselected of the TMD mass ratio $\alpha = 0.03$ is assumed. Then, the optimal TMD parameters β and ξ_{TMD} are tuned using CS as 11%, and 0.91, respectively. For a structure equipped with an ATMD, as a smart structure, an actuator applies a control force to the TMD and its reaction is applied to the top floor story of the structure. In this case, is an 11×1 vector of ones and

$$\mathbf{D} = [0, 0, 0, 0, 0, 0, 0, 0, 0, -1, 1]^{\mathrm{T}}.$$

Considering seismic events as probabilistic events, it is required several time-consuming analyses to access reliable results. In order to overcome this problem, an artificial acceleration of the ground motion is simulated for modelling the possible earthquakes. It is generated by passing a Gaussian White Noise process through filter model proposed by Nagarajaiah and Narasimhan [34].This filter is a modified filter form the well-known Kanai–Tajimi filter. The power spectral density function of the filter is given by:

$$s(\omega) = \frac{4\xi_{\mathrm{g}}\omega_{\mathrm{g}}\omega}{\omega^2 + 24\xi_{\mathrm{g}}\omega_{\mathrm{g}}\omega + \omega_{\mathrm{g}}^2}, \tag{38}$$

in which ξ_g and ω_g are the damping ratio and angular frequency of the ground, respectively. In the study, they considered as $\omega_{\mathrm{g}} = 2\pi\ rad/\mathrm{s}$ and $\xi_{\mathrm{g}} = 0.3$. The output of this filter simulates the earthquake which has been used for design of control system.

Considering the studied structure subjected to the ground artificial acceleration, the optimal modal control gains are tuned by minimizing the cost function described in Eq. (24) for the first three modes of the structures. Different ranges of effective parameters of CS including population size n and the discovery probability P_{a} are tested. The best values of these parameters are given $n = 50$, $P_{\mathrm{a}} = 0.25$. Considering the best result for the first three modes,$\mathbf{G}_{\mathrm{I_{mc}}}$,$\mathbf{G}_{\mathrm{P_{mc}}}$ and $\mathbf{G}_{\mathrm{D_{mc}}}$ are obtained and then the $\mathbf{G}_{\mathrm{mc}}$ is formed as:

$$\mathbf{G}_{\mathrm{mc}} = \begin{bmatrix} 396.125 & 0 & 0 & 15.348 & 0 & 0 & 3.356 & 0 & 0 \\ 0 & 721.332 & 0 & 0 & 8.1087 & 0 & 0 & 1.322 & 0 \\ 0 & 0 & 7.321 & 0 & 0 & 2.011 & 0 & 0 & 0.008 \end{bmatrix}. \tag{39}$$

By substituting $\mathbf{G}_{\mathrm{mc}}$ in Eq. (34), the feedback gain matrix of the proposed LQR-PID controller i.e., $\mathbf{G}_{\mathrm{c}}$ is obtained.

For comparison purposes, a LQR controller is designed for seismic control of the studied structures. The weighting matrix $\mathbf{Q}$ is adopted a diagonal matrix with the following structure.

$$\mathbf{Q} = \begin{bmatrix} \mathbf{K} & \mathbf{0} \\ \mathbf{0} & \mathbf{M} \end{bmatrix}, \tag{40}$$

where $\mathbf{M}$ and $\mathbf{K}$ are the mass and stiffness matrices, respectively. The above form of the $\mathbf{Q}$ matrix represents the sum of the kinetic and strain energies, and it is commonly adopted in structural control applications [27].

Time-history analyses of the structure are carried out using MATLAB/Simulink software [35]. For this purpose, two far-fault earthquakes, El Centro (1940) and Hachinohe (1968), as well as two near-fault earthquakes, Northridge (1994) and Kobe (1995), are considered. The peak ground acceleration (PGA) of theses earthquakes are 0.83, 0.22, 0.34 and 0.82 g. All the above earthquakes have been scaled to the maximum amount of 0.3 g.

Considering the El Centro earthquake, the time histories of the top story displacement and acceleration of the structure equipped with TMD, the structure equipped with ATMD which controlled by LQR and LQR-PID controller, are compared with the corresponding uncontrolled ones in Figs. 3 and 4, respectively. The uncontrolled structure is the structure without passive or active control devices. Also, the time histories of the required control force using these controllers are shown in Fig. 5. It is notable that the first 15 seconds of the structural responses are shown in these figures.

Figures. 3 and 4 indicate that TMD as a passive device reduces the structural responses of the structure subjected to El Centro. Also, it can be seen from these figures that the proposed controller performs better than the LQR in reducing the maximum displacement of the top floor. The LQR and LQR-PID controllers give a reduction of 55% and 62% in comparison with uncontrolled case, respectively. These reductions are given about 42% and 54% in the term of the maximum acceleration of top story. Furthermore, Fig. 5 shows that the maximum required active control force of ATMD for the LQR controller is about 1172 kN while this value is 1232 kN for the LQR-PID controller.

In order to evaluate the performance of the proposed controller during different earthquake excitations, maximum relative displacement and absolute acceleration of the floors of the structure are listed in Tables 1–4 for El Centro, Kobe, Northridge and Hachinohe earthquakes, respectively. The values are for the uncontrolled structure, the structure equipped with TMD as a passive control device, and the structure equipped with ATMD that controlled with the LQR and the LQR-PID controllers.

The results show that the performance of TMDs largely depends on the input earthquake to the structure. For example, TMDs provided the greatest reductions in El Centro earthquakes. But, the least effective is given in Northridge earthquake. Unlike TMD, ATMD can signifi-

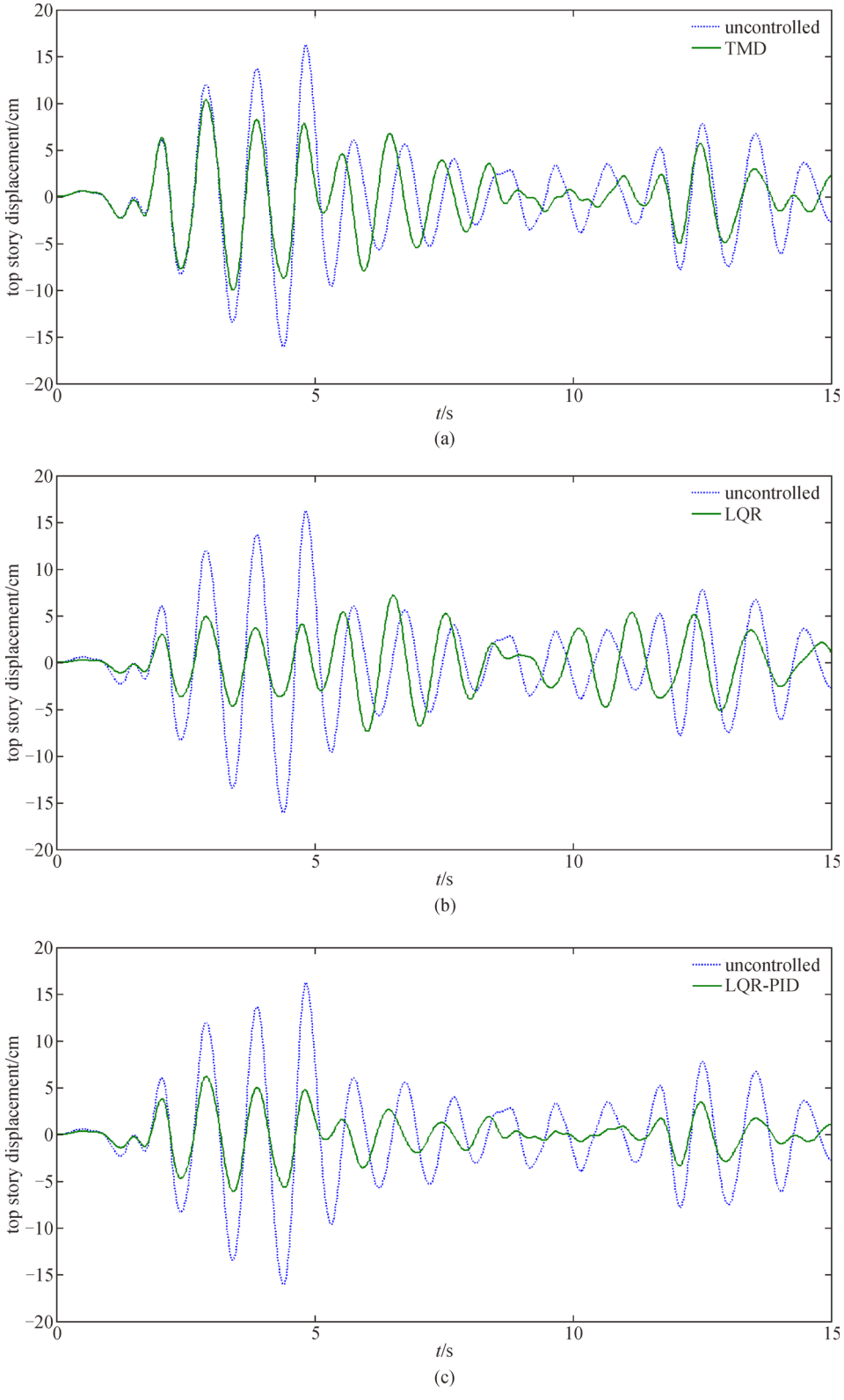

Fig. 3 The time histories of the top story displacement of the structure during El Centro

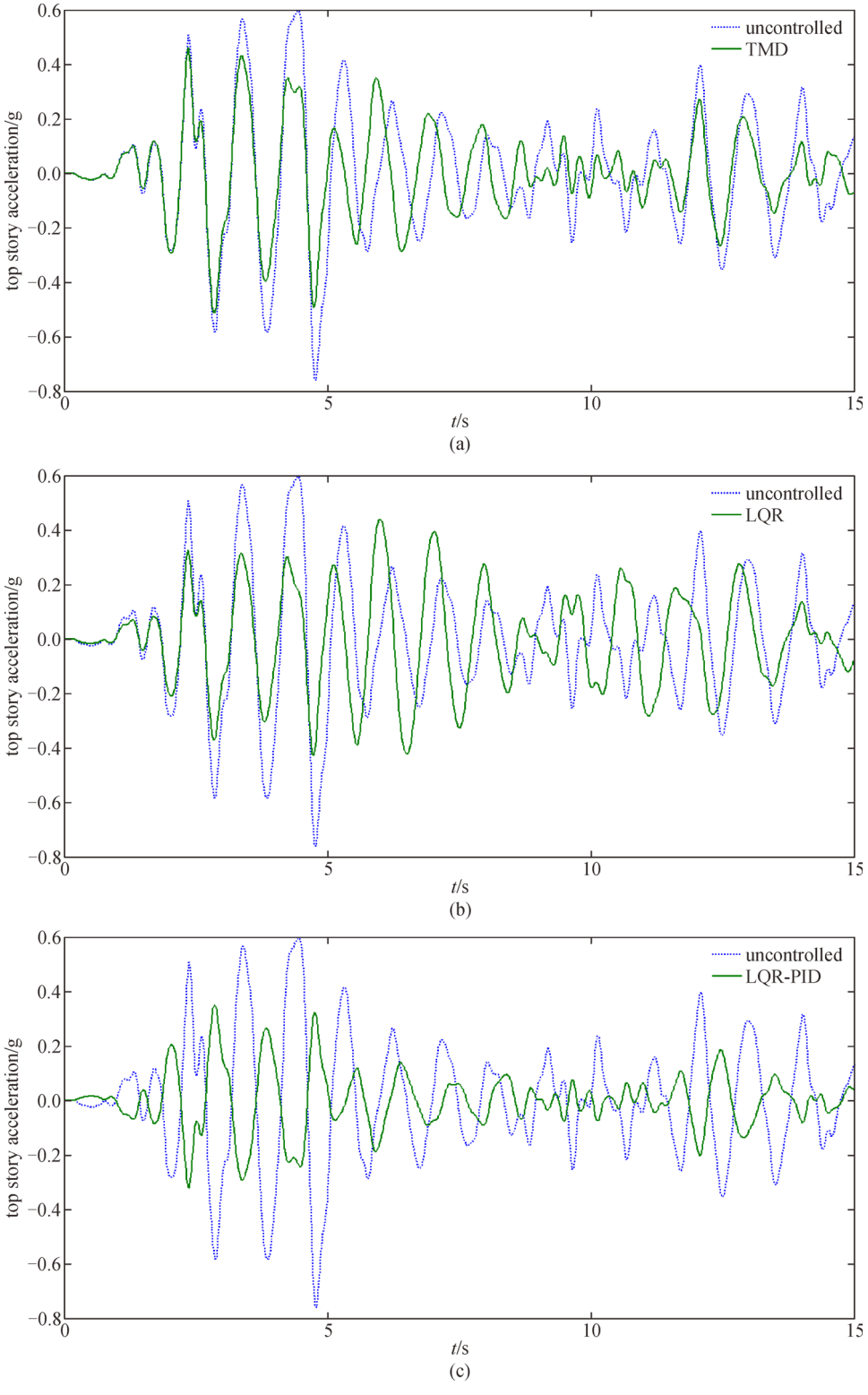

Fig. 4 The time histories of the top story acceleration of the structure during El Centro

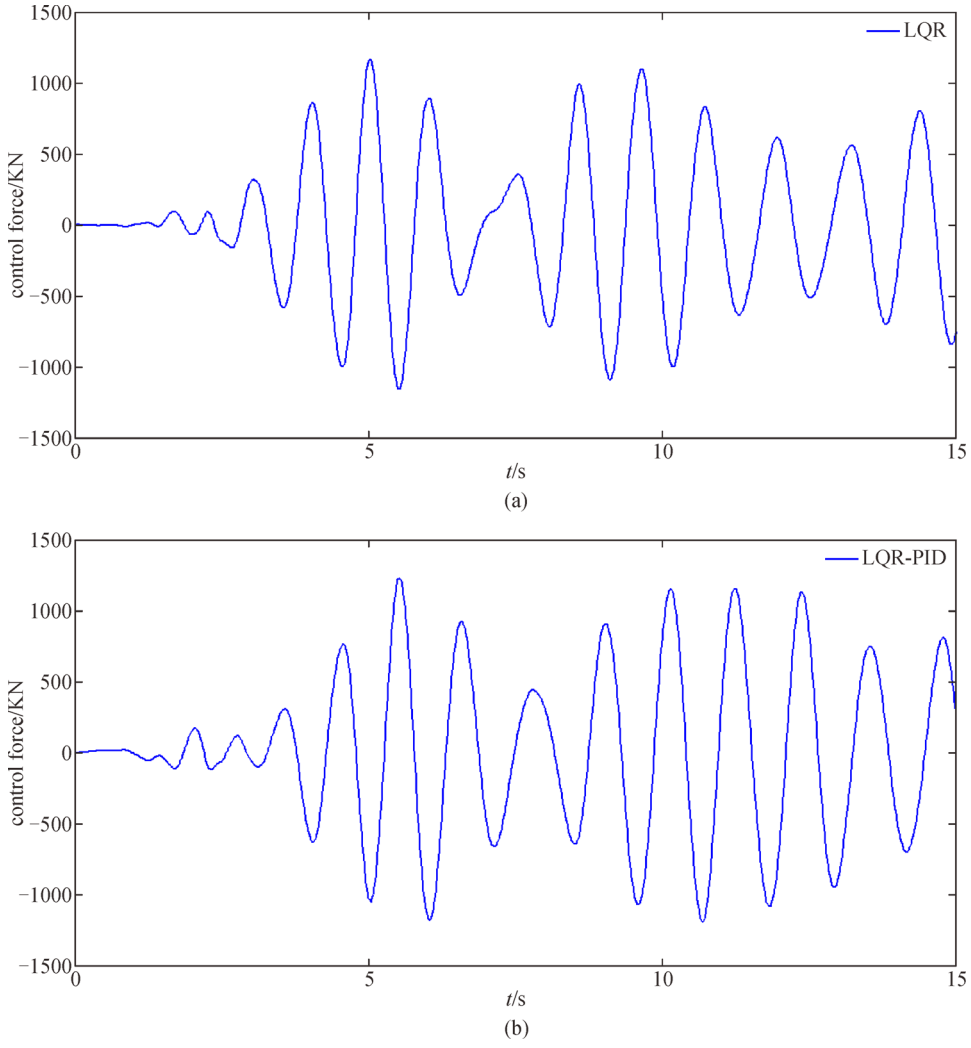

Fig. 5 The time histories of the required control force during El Centro earthquake using LQR and the proposed LQR-PID controllers

Table 1 Maximum structural responses of the structure during El Centro earthquake

maximum relative displacements of floors (cm)					maximum absolute accelerations of floors (g)			
		TMD	ATMD			TMD	ATMD	
floor	unctrl.	passive	LQR	LQR-PID	unctrl.	passive	LQR	LQR-PID
1	2.62	1.61	1.14	0.96	0.26	0.24	0.14	0.11
2	5.13	3.14	2.06	1.68	0.35	0.19	0.20	0.13
3	7.46	4.56	3.18	2.84	0.44	0.31	0.25	0.20
4	9.55	5.83	4.24	3.99	0.50	0.35	0.26	0.20
5	11.37	7.00	5.60	4.39	0.54	0.36	0.28	0.22
6	12.90	8.02	6.19	5.02	0.58	0.33	0.32	0.24
7	14.13	8.93	6.72	5.61	0.60	0.40	0.35	0.28
8	15.12	9.66	6.90	5.90	0.64	0.45	0.34	0.31
9	15.87	10.17	7.11	6.21	0.72	0.49	0.41	0.33
10	16.25	10.43	7.33	6.25	0.76	0.51	0.44	0.35
TMD	-	31.00	47.43	68.41	-	0.52	0.97	1.21

Table 2 Maximum structural responses of the structure during Kobe earthquake

maximum relative displacements of floors (cm)					maximum absolute accelerations of floors (g)			
		TMD	ATMD			TMD	ATMD	
floor	unctrl.	passive	LQR	LQR-PID	unctrl.	passive	LQR	LQR-PID
1	2.66	2.33	1.66	1.40	0.27	0.42	0.22	0.18
2	5.32	4.66	3.33	2.94	0.35	0.29	0.30	0.28
3	7.91	6.92	5.01	4.07	0.44	0.37	0.37	0.31
4	10.37	9.08	6.46	5.16	0.50	0.41	0.42	0.39
5	12.63	11.06	8.21	6.78	0.51	0.41	0.41	0.41
6	14.65	12.83	9.11	8.16	0.58	0.42	0.47	0.49
7	16.36	14.32	10.19	7.91	0.68	0.52	0.56	0.59
8	17.70	15.49	10.97	8.42	0.78	0.61	0.65	0.58
9	18.63	16.30	11.60	9.12	0.85	0.69	0.69	0.68
10	19.11	16.71	12.06	9.74	0.90	0.76	0.75	0.60
TMD	-	41.64	89.54	111.94	-	0.80	1.77	1.82

Table 3 Maximum structural responses of the structure during Northridge earthquake

maximum relative displacements of floors (cm)					maximum absolute accelerations of floors (g)			
		TMD	ATMD			TMD	ATMD	
floor	unctrl.	passive	LQR	LQR-PID	unctrl.	passive	LQR	LQR-PID
1	1.99	1.87	1.53	1.45	0.40	0.27	0.25	0.19
2	3.80	3.57	2.96	2.32	0.49	0.39	0.43	0.31
3	5.35	5.01	4.02	4.23	0.55	0.48	0.47	0.39
4	6.61	6.21	5.41	5.21	0.57	0.53	0.50	0.39
5	7.60	7.13	5.79	5.10	0.53	0.54	0.46	0.34
6	8.31	7.81	6.29	5.31	0.46	0.50	0.39	0.31
7	8.81	8.34	6.84	5.32	0.36	0.42	0.32	0.24
8	9.19	8.86	7.02	6.09	0.42	0.32	0.31	0.27
9	9.51	9.33	7.46	6.21	0.51	0.41	0.36	0.30
10	9.68	9.62	7.49	5.98	0.55	0.49	0.41	0.33
TMD	-	28.87	44.25	54.76	-	0.53	0.91	1.45

Table 4 Maximum structural responses of the structure during Hachinohe earthquake

maximum relative displacements of floors (cm)					maximum absolute accelerations of floors (g)			
		TMD	ATMD			TMD	ATMD	
floor	unctrl.	passive	LQR	LQR-PID	unctrl.	passive	LQR	LQR-PID
1	2.36	2.04	1.51	1.45	0.31	0.30	0.19	0.18
2	4.64	4.03	3.37	3.10	0.39	0.32	0.23	0.25
3	6.79	5.92	4.28	3.78	0.46	0.38	0.30	0.24
4	8.80	7.69	6.23	5.12	0.52	0.47	0.34	0.27
5	10.61	9.33	7.55	5.48	0.54	0.53	0.34	0.28
6	12.20	10.84	8.75	6.18	0.52	0.55	0.32	0.26
7	13.54	12.21	8.64	6.52	0.58	0.53	0.36	0.29
8	14.59	13.35	9.78	7.91	0.68	0.51	0.44	0.39
9	15.30	14.16	10.04	9.12	0.80	0.64	0.49	0.42
10	15.67	14.60	11.13	8.29	0.87	0.76	0.52	0.44
TMD	-	35.04	69.65	82.44	-	0.82	1.43	1.52

cantly control the structural responses in earthquakes with different frequency content. Considering all earthquakes, the results also show that the proposed controller performs better than conventional LQR in the reduction of the maximum displacement and acceleration of stories. For example, the maximum relative displacements of the top story during El Centro earthquake are 7.33 and 6.25 cm for the LQR and the LQR-PID controllers. Similarly, these values in the term of maximum absolute acceleration of the top story are given 0.44 and 0.35 g, respectively. These results show the proposed controller results in a reduction about 15% and 20%, compared to the LQR, in the terms of maximum relative displacements and acceleration of the top story. Considering other earthquakes, the LQR-PID controller reduces the maximum top displacement about 19%, 20% and 26%, in comparison with the LQR, for Kobe, Northridge and Hachinohe earthquakes, respectively. Similarly, these reductions are given about 20%, 20% and 15% in the term of the maximum top acceleration, respectively.

For comparison purposes, the average of the reductions in term of relative displacements and absolute acceleration of all stories, in comparison with the passive TMD, are inserted in Table 5.

Also, the maximum demand control force and mechanical power of ATMD in both LQR and LQR-PID control methods during the studied earthquakes are listed in this table.

Considering the total average of reductions for 4 earthquakes, it can be seen that the proposed controller results in a reduction of 36% and 28% in the terms of displacement and acceleration of the structure while these values are about 25% and 14% for the LQR-PID controller. It can be concluded that the LQR controller is not as effective in reducing the acceleration response as it is in reducing the displacement response, but the proposed controller performs better than LQR in reduction of the peak floors acceleration. Considering the maximum control force of ATMD, it can be seen that the proposed controller has requested relatively more control force in comparison with the LQR controller. However, they have not exceeded the typical practical values. In exchange for this increase, the proposed controller has provided a much better performance for mitigation the seismic responses of the structures. Furthermore, the maximum demand mechanical powers of ATMD for the proposed controller are rather more than the LQR controller. This disadvantage is negligible compared to the significant superiority of the proposed controller in reducing the seismic responses of the studied structures.

A comparison of the frequency responses can indicate the performance of two controllers in the face of earthquakes with different frequency contents. The frequency responses of the studied structure in the terms of top floor displacement and acceleration are shown in Fig. 6. As can be seen, LQR-PID controller decreases the displacement and acceleration of top story, in resonance state, better than the LQR controller. Also, the proposed controller is very effective in the low frequency ranges which have the most input seismic energy.

In the design of the LQR controller, the full state feedback is needed. Therefore, if an integrator is used to convert the measured velocity to the displacement and its integration, 11 sensors and 11 computational resources is required to design the LQR controller. However, the LQR-PID controller reduces them to 1 sensor and 2 computational resources for the structure equipped with ATMD.

8 Conclusions

In order to enhance the performance of the traditional LQR controller, a hybrid controller named LQR-PID controller was proposed in this paper. The proposed LQR-PID controller is a combination of the traditional LQR and the classical PID controllers. To evaluate the performance of the proposed controller, it was applied toward active control of a seismic-excited structure equipped with ATMD. The numerical studies were carried out on a 10-story building equipped with an ATMD. For comparison purposes, a LQR controller is also designed for the structure. An optimization procedure based on CS was

Table 5 Average of reductions of structural responses in comparison with the passive TMD and the maximum demand control force and mechanical power

earthquake	average reduction in relative displacements of floors (%)		average reduction in absolute accelerations of floors (%)		maximum demand control force (kN)		maximum demand mechanical power (kW)	
	LQR	LQR-PID	LQR	LQR-PID	LQR	LQR-PID	LQR	LQR-PID
El Centro	27.71	38.60	17.37	35.54	1172	1232	781	821
Hachinohe	28.32	41.24	1.69	7.90	1204	1298	803	865
Kobe	18.71	28.84	9.72	28.83	1522	1685	1015	1123
Northridge	23.62	37.20	29.20	38.65	816	844	544	563
total average	24.59	36.47	14.50	27.73	1179	1265	786	843

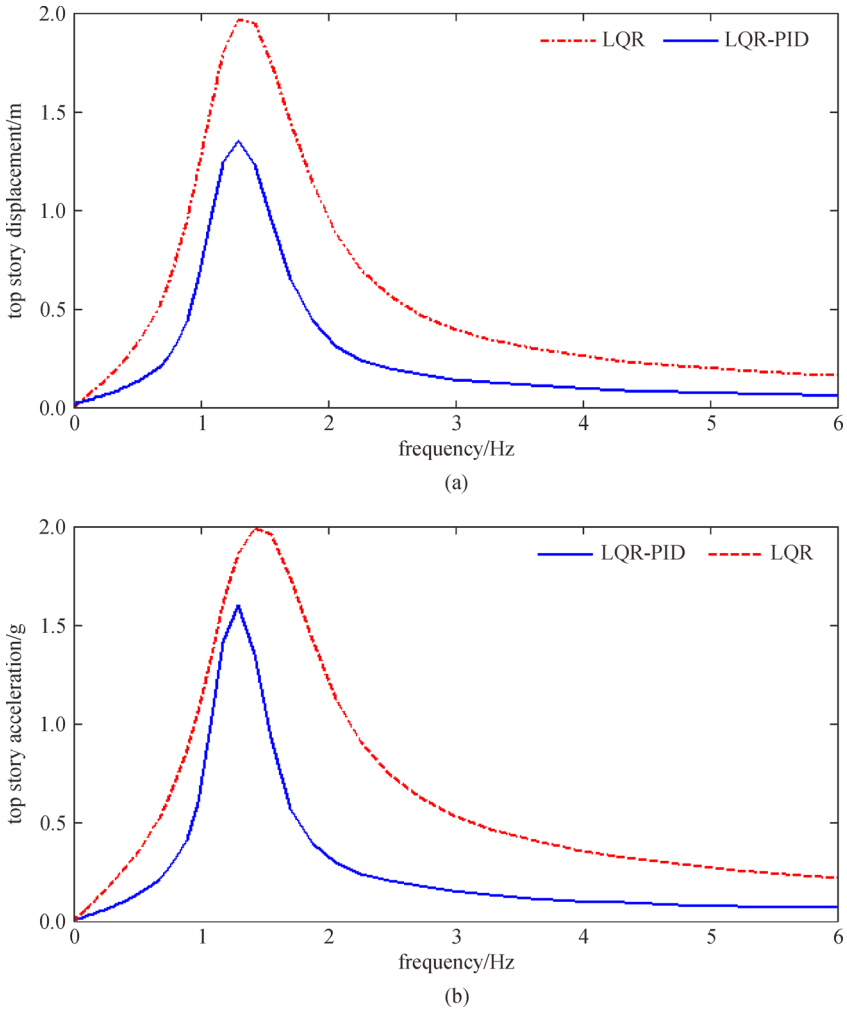

Fig. 6 The frequency responses of the controlled structure using LQR and LQR-PID controller

used for optimum tuning of the modal control gain in a reduced modal space. Considering two far-fault earthquakes and two near-fault earthquakes, the simulation results showed that the hybrid LQR-PID controller performed better than the LQR in terms of reduction of the maximum displacement and the maximum acceleration of the stories of the structure. Considering the total average of reduction for the four studied earthquake, it was concluded that the proposed controller, in comparison with the LQR controller, resulted in a reduction about 16% and 15% in the terms of the maximum displacement and the maximum acceleration of stories at the cost of a small increase in the demanding control force.

References

1. Datta T K. Control of Dynamic Response of Structures. Indo-US Symposium on Emerging Trends in Vibration and Noise Engineering, 1996, 18–20
2. Fisco N R, Adeli H. Smart structures: Part I-Active and semi-active control. Sci Iran, Trans A, 2011, 18(3): 275–284
3. Samali B, Al-Dawod M. Performance of a five-story benchmark model using an active tuned mass damper and a fuzzy controller. Engineering Structures, 2003, 25(13): 1597–1610
4. Samali B, Al-Dawod M, Kwok K C S, Naghdy F. Active control of cross wind response of 76-story tall building using a fuzzy controller. Journal of Engineering Mechanics, 2004, 130(4): 492–498
5. Pourzeynali S, Lavasani H H, Modarayi A H. Active control of high rise building structures using fuzzy logic and genetic algorithms. Engineering Structures, 2007, 29(3): 346–357
6. Huo L, Song G, Li H, Grigoriadis K. H∞robust control design of active structural vibration suppression using an active mass damper. Smart Mater Strut, 2008, 17
7. Fisco N R, Adeli H. Smart structures: Part II—Hybrid control systems and control strategies. Sci Iran, Trans A, 2011, 18(3): 285–295
8. Guclu R, Yazici H, Vibration control of a structure with ATMD against earthquake using fuzzy logic controllers. J Sound Vib, 2008,

318(1-2): 36–49
9. Shen Y, Homaifar A, Chen D. Vibration control of flexible structures using fuzzy logic and genetic algorithms. In: American Control Conference 2000. Chicago, IL, USA, 2000, 1: 448–452
10. Jung W J, Jeong W B, Hong S R, Choi S B. Vibration control of a flexible beam structure using squeeze-mode ER mount. Journal of Sound and Vibration, 2004, 273(1-2): 185–199
11. Fung R F, Liu Y T, Wang C C. Dynamic model of an electromagnetic actuator for vibration control of a cantilever beam with a tip mass. Journal of Sound and Vibration, 2008, 288(4-5): 957–980
12. Guclu R. Fuzzy-logic control of vibrations of analytical multi-degree-of-freedom structural systems. Turk J Eng Environ Sci, 2003, 27(3): 157–167
13. Guclu R. Sliding mode and PID control of a structural system against earthquake. Mathematical and Computer Modelling, 2006, 44(1-2): 210–217
14. Guclu R, Yazici H. Fuzzy-logic control of a non-linear structural system against earthquake induced vibration. Journal of Vibration and Control, 2007, 13(11): 1535–1555
15. Guclu R, Yazici H. Seismic-vibration mitigation of a nonlinear structural system with an ATMD through a fuzzy PID controller. Nonlinear Dynamics, 2009, 58(3): 553–564
16. Aguirre N, Ikhouane F, Rodellar J. Proportional-plus-integral semi active control using magneto- rheological dampers. Journal of Sound and Vibration, 2011, 330(10): 2185–2200
17. Etedali S, Sohrabi M R, Tavakoli S. Optimal PD/PID control of smart base isolated buildings equipped with piezoelectric friction dampers. Earthquake Engineering and Engineering Vibration, 2013, 12(1): 39–54
18. Etedali S, Sohrabi M R, Tavakoli S. An independent robust modal PID control approach for seismic control of buildings. J Civil Eng Urban, 2013, 3(5): 270–291
19. Subasri R, Natarajan A M, Sundaram S, Jianliang W. Neural aided discrete PID active controller for non-linear hysteretic base-isolation building. In: Proceedings of the 9th Asian Control Conference (ASCC). 2013, 1–8
20. Nigdeli S M. Effect of feedback on PID controlled active structures under earthquake excitations. Earthquakes and Structures, 2014, 6 (2): 217–235
21. Yu W, Suresh T, Li X. Stable PID vibration control of building structures. In: Proceedings of the 19th World Congress-International Federation of Automatic Control, South Africa, 2014; 19(1): 4760–4765
22. Etedali S, Tavakoli S, Sohrabi M R. Design of a decoupled PID controller via MOCS for seismic control of smart structures. Earthquakes and Structures, 2016, 10(5): 1067–1087
23. Djajakesukma S L, Samali B, Nguyen H. Study of a semiactive stiffness damper under various earthquake inputs. Earthquake Engineering & Structural Dynamics, 2003, 31(10): 1757–1776
24. Ma T W, Yang T Y. Adaptive feedback–feedforward control of building structures. Journal of Engineering Mechanics, 2004, 130 (7): 786–793
25. Yang J N, Agrawal A K, Samali B, Wu J. Benchmark problem for response control of wind-excited tall buildings. Journal of Engineering Mechanics, 2004, 130(4): 437–446
26. Mei G, Kareem A, Kantor J C. Model predictive control of wind excited building: benchmark study. Journal of Engineering Mechanics, 2004, 130(4): 459–465
27. Alavinasab A, Moharrami H, Khajepour A. Active control of structures using energy-based LQR method. Comput-Aided Civ Inf, 2006, 21(8): 605–611
28. Aldemir U. A simple active control algorithm for earthquake excited structures. Comput-Aided Civ Inf, 2010, 25(3): 218–225
29. Rajabioun R. Cuckoo optimization algorithm. Applied Soft Computing, 2011, 11(8): 5508–5518
30. Gandomi A H, Talatahari S, Yang X S, Deb S. Design optimization of truss structures using cuckoo search algorithm. Struct Des Tall Spec, 2013, 22(17): 1330–1349
31. Civicioglu P, Besdok E A. Conception comparison of the cuckoo search, particle swarm optimization, differential evolution and artificial bee colony algorithms. Artificial Intelligence Review, 2013, 39(4): 315–346
32. Yang X S, Deb S. Cuckoo search: recent advances and applications. Neural Computing & Applications, 2014, 24(1): 169–174
33. Yang X S, Deb S. Cuckoo search via Lévy flights. The World Congress on Nature & Biologically Inspired Computing (NaBIC), 2009, 210–214
34. Nagarajaiah S, Narasimhan S. Smart base-isolated benchmark building part II: phase I, sample controllers for linear and friction isolation. J Struct Control Hlth, 2006, 13(2-3): 589–604
35. MATLAB. The Math Works. Inc, Natick, MA, 2000